Int. J. Heat Mass Transfer. Vol. 11, pp. 709–719. Pergamon Press 1968. Printed in Great Britain

ON THE DYNAMICS OF HEMISPHERICAL PHASE GROWTH IN NONUNIFORM CONCENTRATION FIELDS

H. Y. CHEH* and CHARLES W. TOBIAS
Inorganic Materials Research Division, Lawrence Radiation Laboratory, and
Department of Chemical Engineering, University of California, Berkeley, U.S.A.

(*Received* 22 *March* 1967 *and in revised form* 7 *July* 1967)

Abstract—Theoretical calculations on the dynamics of asymptotic bubble growth in an initially nonuniform concentration field are performed. A significant simplification is achieved by noting that the Jakob number for mass transfer is usually small so that the convective transport can be neglected in comparison with the diffusive transport. Numerical solutions are obtained for the growth rate of a hemispherical bubble on a surface with linear and exponential initial concentration fields of the supersaturated gas in the diffusion boundary layers and also for the cases involving concentration fields resulting from the constant interfacial concentration and the constant mass flux experiments.

NOMENCLATURE

A, interfacial area between two phases [cm^2];
D, diffusivity of a species in a homogeneous medium [cm^2/s];
J, Jakob number for mass transfer,
$$= 1/\rho_v \int_0^\pi [f(0,\theta) - c_s] \sin\theta \, d\theta;$$
R, radius of a bubble [cm];
V, volume of a bubble [cm^3];
c, concentration of a species [g/cm^3];
f, an initial concentration field for bubble growth [g/cm^3];
g, a dimensionless concentration,
$$= \frac{\int_0^\pi [f(m,\theta) - c_s] \sin\theta \, d\theta}{\int_0^\pi [f(0,\theta) - c_s] \sin\theta \, d\theta};$$
m, a dimensionless distance coordinate, $= r - R/\ell$;
q, a constant flux of mass [g/cm^{2}s];
t, time [s];
$\mathscr{J}$, a modified Jakob number, $= (J/2\pi)^{\frac{1}{2}}$;
ℓ, a characteristic length [cm];
$\mathscr{R}$, a dimensionless radius, $= R/\ell$.

Greek symbols

ξ, a dimensionless parameter, $= (2J\tau)^{\frac{1}{2}}$;
ρ, density of a fluid [g/cm^3];
τ, a dimensionless time, $= Dt/\ell^2$;
ω, a dimensionless concentration,
$$= \frac{\text{interface concentration} - \text{bulk concentration}}{\text{interface concentration} - \text{saturation concentration}}.$$

Subscripts

q, refers to the case of constant mass flux;
s, refers to quantities at saturation;
v, refers to quantities in the vapor or gas phase;
∞, refers to quantities in bulk medium.

1. INTRODUCTION

THE DYNAMICS of phase growth is of importance to many practical processes. For instance, the growth of bubbles is essential in understanding the overall mass- or heat-transfer aspects in electrolytic gas evolution or in nucleate boiling, respectively.

The growth of gas bubbles on electrodes is controlled by mass transfer with supersaturation serving as driving force whereas the growth of vapor bubbles in nucleate boiling is controlled by heat transfer with superheat as driving force.

* Present address: Bell Telephone Laboratories, Murray Hill, N.J., U.S.A.

A numerical evaluation for the dynamics of bubble growth involves solving simultaneously the equation of continuity, the equation of motion and either the equation of convective diffusion for electrolytic gas evolution or the equation of heat flow for nucleate boiling. An exact solution is often too complex to be obtained. Reasonable assumptions based on a careful examination of a physical process are often used to simplify the individual problem.

It was found by Plesset and Zwick [1], Forster and Zuber [2], Scriven [3] and Glas and Westwater [4] that for all practical purposes, the consideration of the asymptotic stage of growth where viscous, inertia and surface forces can all be neglected in the extended Rayleigh equation of motion is adequate for describing bubble growth. The growth of very small bubble is usually slow due to the high surface force that arrests its radial motion. However, the transition from this slow growth to the asymptotic growth occurs in a very short time (approximately 10^{-2} s) [5]. It is, therefore, only this later stage which provides practical interest.

At this asymptotic stage, the extended Rayleigh equation reduces to a trivial equation which states that the pressure inside the bubble is equal to the pressure in the liquid. Only the convective diffusion equation or the equation of heat flow need to be solved for the bubble dynamics.

Epstein and Plesset [6] calculated the growth of a gas bubble in a uniformly supersaturated solution. The problem was greatly simplified by their assumption that the diffusion boundary layer was so thick that the convective transport can be neglected. Methods that include the convective transport at very rapid bubble growth in nucleate boiling have been developed by Plesset and Zwick [1] and also by Forster and Zuber [2]. Plesset and Zwick calculated the dynamics of spherical vapor phase growth using a thin thermal boundary-layer approximation and the method of regular perturbation. Forster and Zuber considered the bubble as a spherically distributed heat sink and solved also for the dynamics of bubble growth at the asymptotic stage. Griffith [7] solved the case of a hemispherical bubble growing in a linear temperature field whereas Bankoff [8] solved the bubble dynamics at the surface of an exponentially heated plate. An exact calculation using the method of similarity transform for the case of asymptotic growth in an initially uniform concentration or temperature field was obtained by Birkhoff *et al.* [9] and also by Scriven [3]. This exact solution reduces to Epstein and Plesset's result at low growth rate and to Plesset and Zwick's result at high growth rate. The numerical constant in Forster and Zuber's calculation is 9·3 per cent lower than the exact solution. Skinner and Bankoff [10], using the regular perturbation approach of Plesset and Zwick, established a parametric solution for the asymptotic bubble growth in general temperature fields at large superheat.

In this paper, we shall treat the case of a gas bubble growing in an initially nonuniform concentration field.

2. THEORETICAL ANALYSIS

We are dealing with a hemispherical bubble growing asymptotically on a surface in an initially axisymmetrical concentration field. Both phases are considered to be incompressible. Constant fluid density and constant mass diffusivity are assumed. The density of the gas phase is considered negligible when compared to the liquid density. The diffusion boundary layer is assumed to be so thick that convective transport can be neglected. The transport of solute by motion of the liquid phase is neglected. The solution is therefore applicable to relatively slow rate of growth.

A general solution of the spherically symmetric case will first be derived. The solution for the axisymmetric case will then be obtained through a transformation which reduces the axisymmetric equation to the spherically symmetric form. The general result will then be applied to several practical problems [11].

A. *Spherically symmetric case*

This is the case where bubbles are assumed to be growing in a concentration field which is spherically symmetrical. Figure 1 shows the hypothetical concentration field in the solution before the formation of a bubble. Figure 2 gives the schematic concentration field around the bubble during its growth.

The solution to equation (1) subjected to boundary conditions equations (2) and (3) can be found in Carslaw and Jaeger [12]:

$$c = \frac{1}{2r\sqrt{(\pi Dt)}}\int_R^\infty r'f(r')\{\exp[-(r-r')^2/4Dt] - \exp[-(r+r'-2R)^2/4Dt]\}\,dr' + c_s\frac{R}{r}\operatorname{erf}\frac{r-R}{2\sqrt{(Dt)}}. \quad (5)$$

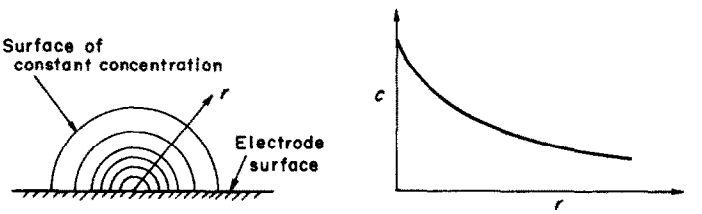

FIG. 1. Initial concentration field for the spherically symmetric case.

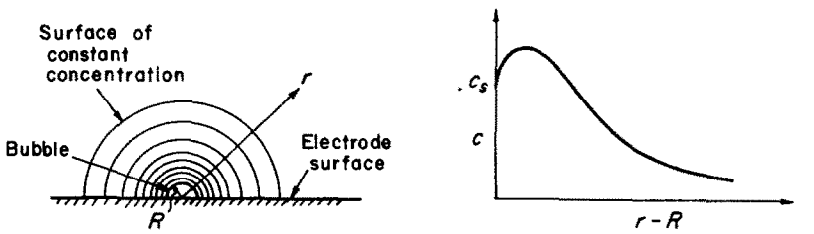

FIG. 2. Schematic diagram for the concentration field for the spherically symmetric case.

The diffusion equation in spherical coordinates for this case is

$$\frac{\partial c}{\partial t} = \frac{D}{r^2}\frac{\partial}{\partial r}\left(r^2\frac{\partial c}{\partial r}\right). \quad (1)$$

The boundary conditions are

1. at $t = 0$, $r \geqslant 0$, $c = f(r)$, (2)
2. at $r = R$, $t > 0$, $c = c_s$, (3)
3. at $r = R$, $t > 0$,

a mass balance gives

$$\rho_v\frac{dV}{dt} = AD\left(\frac{\partial c}{\partial r}\right)_{r=R},$$

or

$$\rho_v\frac{dR}{dt} = D\left(\frac{\partial c}{\partial r}\right)_{r=R}. \quad (4)$$

Differentiating equation (5) with respect to r and letting $r = R$, combining with equation (4), we obtain an integro-differential equation for the bubble history,

$$\rho_v\frac{dR}{dt} = D\left[\frac{1}{2R\sqrt{(\pi Dt)}}\int_R^\infty r'f(r') \times \frac{(r'-R)}{Dt}\exp[-(r'-R)^2/4Dt]\,dr' - c_s\left(\frac{1}{R}+\frac{1}{\sqrt{(\pi Dt)}}\right)\right]. \quad (6)$$

This can be nondimensionalized by letting

$$m = \frac{r-R}{\ell}, \quad \mathscr{R} = \frac{R}{\ell},$$

$$\tau = \frac{Dt}{\ell^2} \quad \text{and} \quad g(m) = \frac{f(m) - c_s}{f(0) - c_s}, \tag{7}$$

to give a more convenient form,

$$\frac{d\mathscr{R}}{d\tau} = \frac{J}{2\mathscr{R}\sqrt{(\pi\tau^3)}} \int_0^\infty (m + \mathscr{R}) g(m)\, m \times \exp(-m^2/4\tau)\, dm, \tag{8}$$

where $J = \{[f(0) - c_s]/\rho_v\}$ is the Jakob number for mass transfer.

B. *Axisymmetric case*

The spherically symmetric case in the presence of a planar surface is a hypothetical one. The concentration field is usually of axisymmetric nature. Using spherical coordinates, this means there is no dependence of ϕ. Figure 3 shows the initial concentration field and Fig. 4 is a schematic picture of the concentration field during the bubble growth.

The diffusion equation for this case is

$$\frac{\partial c}{\partial t} = D\left[\frac{1}{r^2}\frac{\partial}{\partial r}\left(r^2\frac{\partial c}{\partial r}\right) + \frac{1}{r^2 \sin\theta}\frac{\partial}{\partial\theta}\left(\sin\theta\frac{\partial c}{\partial\theta}\right)\right]. \tag{9}$$

The boundary conditions are

1. at $t = 0$, $r \geq 0$, $c = f(r, \theta)$, (10)
2. at $r = R$, $t > 0$, $c = c_s$, (11)
3. at $r = R$, $t > 0$,

$$\rho_v \frac{dR}{dt} = \frac{D}{2}\int_0^\pi \left(\frac{\partial c}{\partial r}\right)_{r=R} \sin\theta\, d\theta. \tag{12}$$

This set of equations can be transformed to the same form as that of the spherically symmetric case by letting

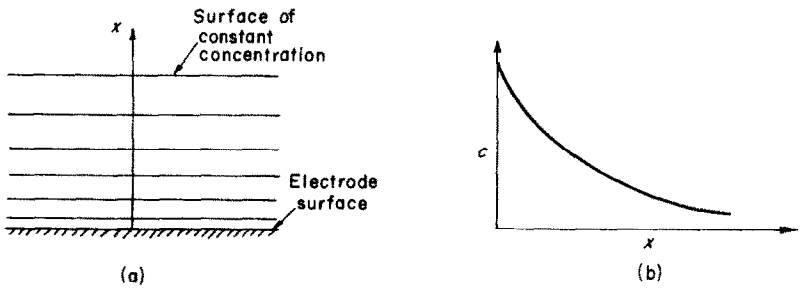

FIG. 3. Initial concentration field for the axisymmetric case. (Axisymmetric with respect to x-axis.)

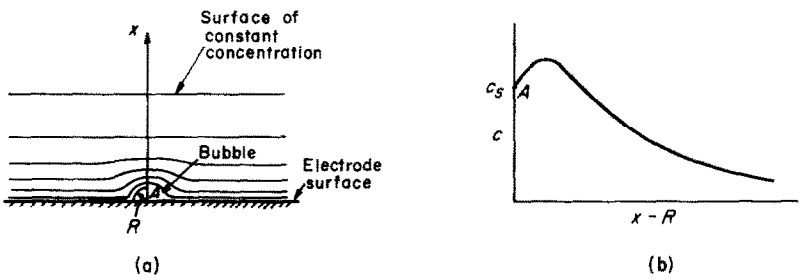

FIG. 4. Schematic diagram for the concentration field for the axisymmetric case. (Axisymmetric with respect to x-axis.)

$$c'(r,t) = \frac{\int_0^\pi [c(r,\theta,t) - c_s] \sin\theta \, d\theta}{\int_0^\pi [f(0,\theta) - c_s] \sin\theta \, d\theta}. \quad (13)$$

In terms of c', equations (9–12) are

$$\frac{\partial c'}{\partial t} = \frac{D}{r^2}\frac{\partial}{\partial r}\left(r^2 \frac{\partial c'}{\partial r}\right), \quad (14)$$

and

1. at $t = 0, \quad r \geqslant 0,$

$$c' = \frac{\int_0^\pi [f(r,\theta) - c_s] \sin\theta \, d\theta}{\int_0^\pi [f(0,\theta) - c_s] \sin\theta \, d\theta}, \quad (15)$$

2. at $r = R, \quad t > 0, \quad c' = 0, \quad (16)$

3. at $r = R, \quad t > 0,$

$$\rho_v \frac{dR}{\partial t} = D\left(\frac{\partial c'}{\partial r}\right)_{r=R}. \quad (17)$$

Comparing equations (1) and (2–4) to equations (14) and (15–17), it is obvious that equation (8) is also valid for the axisymmetric case provided $g(m)$ and J are redefined as

$$g(m) = \frac{\int_0^\pi [f(m,\theta) - c_s] \sin\theta \, d\theta}{\int_0^\pi [f(0,\theta) - c_s] \sin\theta \, d\theta}, \quad (18)$$

and

$$J = \frac{1}{\rho_v}\int_0^\pi [f(0,\theta) - c_s] \sin\theta \, d\theta. \quad (19)$$

C. *Solutions*

The radius–time history for the bubble may be obtained for various cases by solving equation (8) with the appropriate initial conditions $g(m)$. An exact solution will be presented for the case of uniform initial supersaturation. For cases of general initial conditions, no exact solutions can be obtained. The solution for cases of low and of high Jakob numbers will then be given.

1. *Uniform supersaturation.* $g(m)$ for this case is simply unity. Equation (8) is, therefore,

$$\frac{d\mathscr{R}}{d\tau} = \frac{1}{2\mathscr{R}\sqrt{(\pi\tau^3)}}\int_0^\infty (m + \mathscr{R}) m \exp(-m^2/4\tau)\, dm$$

$$= J\left[\frac{1}{\mathscr{R}} + \frac{1}{\sqrt{(\pi\tau)}}\right]. \quad (20)$$

If we let $\xi^2 = 2J\tau$ and $\mathscr{J} = (J/2\pi)^{\frac{1}{2}}$, equation (20) simplifies to

$$\frac{d\mathscr{R}}{d\xi} = \frac{1}{\mathscr{R}} + 2\mathscr{J}. \quad (21)$$

If the degree of supersaturation is low, $2\mathscr{J}$ will be much smaller than $1/\mathscr{R}$. This is equivalent to saying that

$$\int_0^\infty m^2 \exp(-m^2/4\tau)\, dm$$

is much larger than

$$\int_0^\infty \mathscr{R} m \exp(-m^2/4\tau)\, dm.$$

The solution is then simply

$$\mathscr{R} = (2J\tau)^{\frac{1}{2}}, \quad (22)$$

or

$$R = \sqrt{\left(\frac{2D(c_\infty - c_s)}{\rho_v} t\right)}. \quad (23)$$

If the degree of supersaturation is very high, i.e. $2\mathscr{J} \gg 1/\mathscr{R}$ or

$$\int_0^\infty m^2 \exp(-m^2/4\tau)\, dm$$

is much smaller than

$$\int_0^\infty \mathscr{R} m \exp(-m^2/4\tau)\, dm,$$

the solution is

$$\mathscr{R} = \frac{2}{\sqrt{(\pi)}} J\tau^{\frac{1}{2}}, \quad (24)$$

or

$$R = \frac{2}{\sqrt{(\pi)}} \frac{c_\infty - c_s}{\rho_v} \sqrt{(Dt)}. \quad (25)$$

Equations (23) and (25) are the same as those calculated by Epstein and Plesset [6]. A complete solution to equation (21) has also been obtained by them. Their result can be expressed as

$$\mathscr{R} = e^{\mathscr{J}z}\{\cosh[(1+\mathscr{J}^2)^{\frac{1}{2}}z] + \mathscr{J}(1+\mathscr{J}^2)^{-\frac{1}{2}}\sinh[(1+\mathscr{J}^2)^{\frac{1}{2}}z]\}, \quad (26)$$

$$\xi = e^{\mathscr{J}z}(1+\mathscr{J}^2)^{-\frac{1}{2}}\sinh[(1+\mathscr{J}^2)^{\frac{1}{2}}z]. \quad (27)$$

2. *Low supersaturation.* This is the case where in equation (8),

$$\int_0^\infty m^2 g(m)\exp(-m^2/4\tau)\,dm$$

is much greater than

$$\int_0^\infty \mathscr{R} m g(m)\exp(-m^2/4\tau)\,dm.$$

Equation (8), therefore, reduces to

$$\frac{d\mathscr{R}}{d\tau} = \frac{1}{2\mathscr{R}\sqrt{(\pi\tau^3)}}\int_0^\infty m^2 g(m)\exp(-m^2/4\tau)\,dm, \quad (28)$$

which can be integrated to give

$$\mathscr{R}^2 = 2J\int_0^\infty m g(m)\operatorname{erfc}\frac{m}{2\tau^{\frac{1}{2}}}\,dm. \quad (29)$$

This is the basic solution for the low supersaturation case. It will now be applied to several practical cases.

a. *Linear concentration field.* A linear decay of concentration from the surface to the distance ℓ and constant thereafter has often been used in literature in performing mass-transfer calculations. This distribution can be given in spherical coordinates by

$$f(r,\theta) = \begin{cases} c_\infty + (c_w - c_\infty)\left(1 - \dfrac{r\cos\theta}{\ell}\right), & r/\ell < 1, \quad (30) \\ c_\infty, \quad 0 < \theta < \cos^{-1}\dfrac{\ell}{r}, & \\ c_\infty + (c_w - c_\infty)\dfrac{r\cos\theta}{\ell}, \quad \cos^{-1}\dfrac{\ell}{r} < \theta < \dfrac{\pi}{2}, & r/\ell > 1, \quad (31),\ (32) \end{cases}$$

where c_∞ is the bulk concentration and c_w is the concentration at $\theta = \pi/2$. Substituting equations (30–32) into equation (18) yields

$$g(m) = \begin{cases} 1 - \omega\left(1 - \dfrac{1}{2m}\right), & m > 1, \quad (33) \\ 1 - \dfrac{\omega m}{2}, & m < 1, \quad (34) \end{cases}$$

where

$$\omega = \frac{c_w - c_\infty}{c_w - c_s}. \quad (35)^*$$

Substituting equations (33) and (34) into equation (29) and integrating, the following analytic solution is obtained,

$$\mathscr{R}^2 = 2J\left[\tau - \omega\left\{\frac{1}{6}\operatorname{erfc}\frac{1}{2\tau^{\frac{1}{2}}} + \tau\operatorname{erfc}\frac{1}{2\tau^{\frac{1}{2}}} + \frac{4\tau^{\frac{3}{2}}}{3\sqrt{(\pi)}}\left[1 - \left(1 + \frac{1}{4\tau}\right)\exp\left(-\frac{1}{4\tau}\right)\right]\right\}\right]. \quad (36)$$

This result is given in Fig. 5. For cases where $\omega > 1$, a maximum of radius occurs. The growth of bubble is followed by a collapse which is due to the low concentration of gas in the bulk solution.

b. *Exponential concentration field.* A better approximation to the linear concentration field in the diffusion boundary layer is the exponential representation, i.e.

* ω will again appear in later cases. It can be expressed more generally by

$$\omega = \frac{\text{interface concentration–bulk concentration}}{\text{interface concentration–saturation concentration}}.$$

Therefore, $\omega = 0$ signifies the uniform supersaturation case. $0 < \omega < 1$ means that the solution is supersaturated, however, a gradient of concentration from the bulk to the interface exists. $\omega = 1$ means the bulk solution is saturated and $\omega > 1$ is the case where the bulk is below saturation.

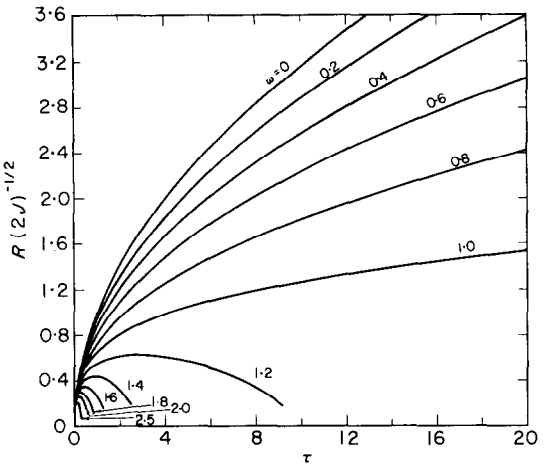

FIG. 5. Low supersaturation with an initially linear concentration field.

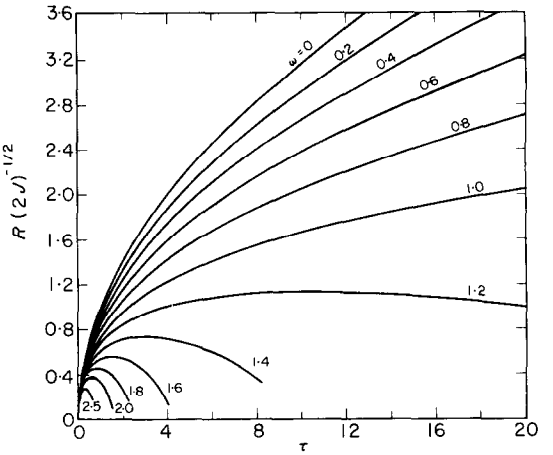

FIG. 6. Low supersaturation with an initially exponential concentration field.

$$f(r,\theta) = c_\infty + (c_w - c_\infty)\exp\left(\frac{r\cos\theta}{-\ell}\right), \quad 0 < \theta < \frac{\pi}{2}, \tag{37}$$

or

$$g(m) = 1 - \omega\left[1 - \frac{1}{m}(1 - e^{-m})\right], \tag{38}$$

where $\omega = (c_w - c_\infty)/(c_w - c_s)$. Equation (29) can also be integrated in closed form for this case,

$$\mathscr{R}^2 = 2J\left[\tau - \omega\left(\tau - \frac{2}{\sqrt{(\pi)}}\tau^{\frac{1}{2}} - 1 - e^{\tau}\operatorname{erfc}\tau^{\frac{1}{2}}\right)\right]. \tag{39}$$

A numerical solution is given in Fig. 6.

c. *Constant interfacial concentration.** The interfacial concentration c_w is maintained to be a constant. The well-known solution of the diffusion equation prior to the appearance of a bubble in a semi-infinite medium provides us the initial condition for this case [12],

$$f(r,\theta) = c_\infty + (c_w - c_\infty)\operatorname{erfc}\frac{x}{2\sqrt{(Dt)}}$$

$$= c_\infty + (c_w - c_\infty)\operatorname{erfc}\frac{r\cos\theta}{\ell}, 0 < \theta < \frac{\pi}{2}, \tag{40}$$

where $\ell = 2(Dt)^{\frac{1}{2}}$ and t can be interpreted as the waiting time for bubble growth as is often done in the literature of nucleate boiling. Integrating equation (18), $g(m)$ is obtained as,

$$g(m) = 1 - \omega\left[\operatorname{erf} m - \frac{1}{(\sqrt{\pi})m} \times [1 - \exp(-m^2)]\right]. \tag{41}$$

The bubble history is, therefore,

$$\mathscr{R}^2 = 2J\int_0^\infty m\left[1 - \omega\left(\operatorname{erf} m - \frac{1}{(\sqrt{\pi})m} \times [1 - \exp(-m^2)]\right)\right]\operatorname{erfc}\frac{m}{2\tau^{\frac{1}{2}}}\,dm. \tag{42}$$

A numerical solution is given in Fig. 7.

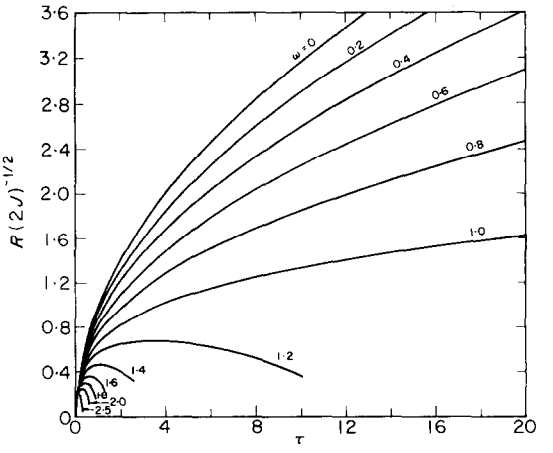

FIG. 7. Low supersaturation for the case of constant interfacial concentration.

* This corresponds to the case of constant potential in electrolytic gas evolution.

d. *Constant mass flux.** The initial condition for this case is [12],

$$f(r,\theta) = c_\infty + q\sqrt{\left(\frac{4t}{D}\right)}\, i\,\mathrm{erfc}\frac{x}{2\sqrt{(Dt)}}$$

$$= c_\infty + c_q\, i\,\mathrm{erfc}\frac{r\cos\theta}{\ell}, 0 < \theta < \frac{\pi}{2}, \qquad (43)$$

where q is the constant mass flux, $c_q = q(4t/D)^{\frac{1}{2}}$ and $\ell = 2(Dt)^{\frac{1}{2}}$. $g(m)$ for this case is

$$g(m) = 1 - \omega\left[1 - \exp(-m^2) + \frac{\sqrt{(\pi)}}{2}m \times \mathrm{erfc}\, m - \frac{1}{2m}\gamma\left(\frac{3}{2}, m^2\right)\right], \qquad (44)$$

where

$$\omega = \frac{c_q/\sqrt{(\pi)}}{c_\infty + \frac{c_q}{\sqrt{(\pi)}} - c_s}.$$

The bubble history is, therefore,

$$\mathscr{R}^2 = 2J\int_0^\infty m\left\{1 - \omega\left[1 - \exp(-m^2) + \frac{\sqrt{(\pi)}}{2}m\,\mathrm{erfc}\, m - \frac{1}{2m}\gamma\left(\frac{3}{2}, m^2\right)\right]\right\} \times \mathrm{erfc}\frac{m}{2\tau^{\frac{1}{2}}}\,\mathrm{d}m. \qquad (45)$$

A numerical solution is given in Fig. 8.

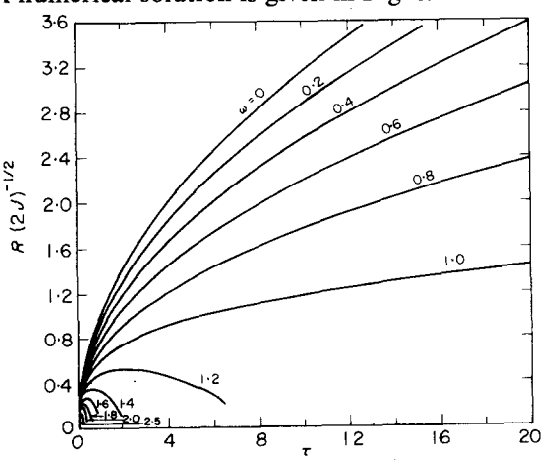

FIG. 8. Low supersaturation for the case of constant mass flux.

* This corresponds to the case of constant current in electrolytic gas evolution.

3. *High supersaturation.* This is the case where

$$\int_0^\infty \mathscr{R}mg(m)\exp(-m^2/4\tau)\,\mathrm{d}m$$

is much greater than

$$\int_0^\infty m^2 g(m)\exp(-m^2/4\tau)\,\mathrm{d}m.$$

Equation (8) thus reduces to

$$\frac{\mathrm{d}\mathscr{R}}{\mathrm{d}\tau} = \frac{J}{2\sqrt{(\pi\tau^3)}}\int_0^\infty mg(m)\exp(-m^2/4\tau)\,\mathrm{d}m, \qquad (46)$$

which can be integrated to give

$$\mathscr{R} = J\int_0^\infty g(m)\,\mathrm{erfc}\frac{m}{2\tau^{\frac{1}{2}}}\,\mathrm{d}m. \qquad (47)$$

This equation is applied to the same cases treated in the last section. We shall merely give the bubble-history equation whose numerical solutions are presented in Figs. 9–12.

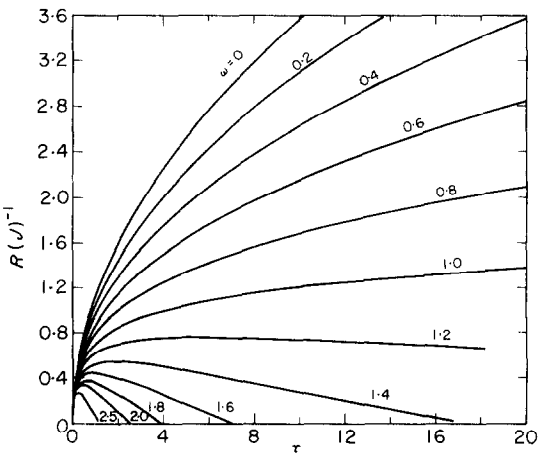

FIG. 9. High supersaturation with an initially linear concentration field.

a. Linear concentration field

$$\mathscr{R} = J\left[\frac{2}{\sqrt{(\pi)}}\tau^{\frac{1}{2}} - \omega\left(\int_0^1 \frac{m}{2}\,\mathrm{erfc}\frac{m}{2\tau^{\frac{1}{2}}}\,\mathrm{d}m + \int_1^\infty \left(1 - \frac{1}{2m}\right)\mathrm{erfc}\frac{m}{2\tau^{\frac{1}{2}}}\,\mathrm{d}m\right)\right]. \qquad (48)$$

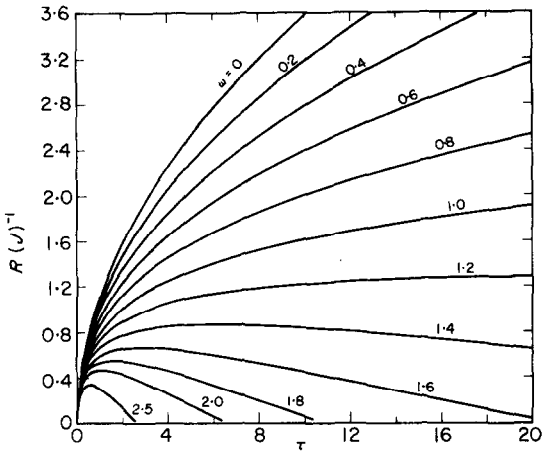

FIG. 10. High supersaturation with an initially exponential concentration field.

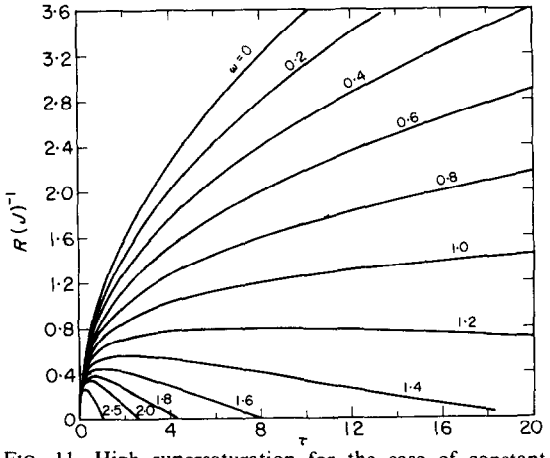

FIG. 11. High supersaturation for the case of constant interfacial concentration.

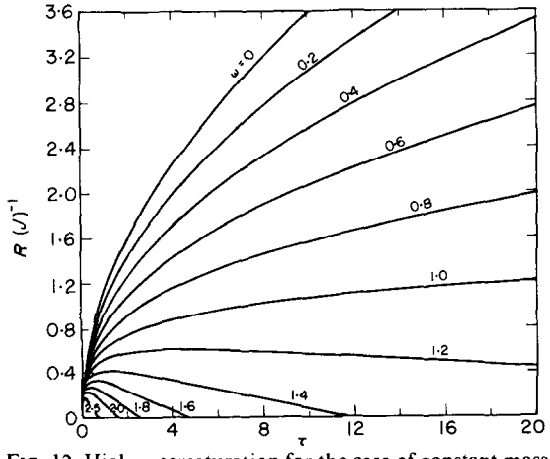

FIG. 12. High supersaturation for the case of constant mass flux.

b. Exponential concentration field

$$\mathscr{R} = J\int_0^\infty \left[1 - \omega\left(1 - \frac{1}{m}(1 - e^{-m})\right)\right] \times \operatorname{erfc}\frac{m}{2\tau^{\frac{1}{2}}}\,dm. \tag{49}$$

c. Constant interfacial concentration

$$\mathscr{R} = J\int_0^\infty \left[1 - \omega\left(\operatorname{erf} m - \frac{1}{(\sqrt{\pi})m} \times [1 - \exp(-m^2)]\right)\right] \operatorname{erfc}\frac{m}{2\tau^{\frac{1}{2}}}\,dm. \tag{50}$$

d. Constant mass flux

$$\mathscr{R} = J\int_0^\infty \left\{1 - \omega\left[1 - \exp(-m^2) + \frac{\sqrt{(\pi)}}{2} m \operatorname{erfc} m - \frac{1}{2m}\gamma\left(\frac{3}{2}, m^2\right)\right]\right\} \times \operatorname{erfc}\frac{m}{2\tau^{\frac{1}{2}}}\,dm. \tag{51}$$

Thus we have completed our calculation for the bubble dynamics under the condition that the convective transport can be neglected. It is found that for the case of uniform supersaturation, the radius is proportional to $(Dt)^{\frac{1}{2}}$ for both the low and the high supersaturation cases. However, the dependence of $\mathscr{R}$ on the dimensionless driving force, J, is different. It is proportional to $J^{\frac{1}{2}}$ for the case of low supersaturation and to J for the high supersaturation case. For other cases, the dependence on J remains the same as the uniform supersaturation case. However, the radius of the bubble is no longer proportional to $(Dt)^{\frac{1}{2}}$.

Since no generation term is considered in the derivation, the bubble cannot grow indefinitely. For cases where $\omega \leqslant 1$, the growth will cease after the bubble has completely exhausted the supersaturated concentration in the solution. For cases where $\omega > 1$, a collapse often occurs due to the low gas content in the bulk solution.

3. DISCUSSION

Westerheide and Westwater [13] and also Glas and Westwater [4] measured the growth of various kinds of gas bubbles during electrolysis. For the majority of bubbles they studied, the radius of the bubble was found to be proportional to the square root of time. From the radius–time plot, using Scriven's solution [3] for the asymptotic growth of bubble in a uniformly supersaturated solution, these authors calculated the supersaturation ratio defined as c_∞/c_s for these various types of gas bubbles. Extensive results tabulated in Glas' dissertation [14] are summarized in Table 1.

Table 1. *Various supersaturation ratios reported by Glas* [14]

Gas	c_s* in water at 25°C, 1 atm mol/cc	Average c_∞/c_s	Number of bubbles used in averaging
Hydrogen	$7{\cdot}13 \times 10^{-7}$	4·65	433
Oxygen	$11{\cdot}4 \times 10^{-7}$	5·67	21
Chlorine	$8{\cdot}15 \times 10^{-5}$	1·09	86
Carbon dioxide	$3{\cdot}00 \times 10^{-5}$	1·31	112

* c_s's are taken from LANDOLT–BORNSTEIN, *Zählenwerte und Funktionen*, 6. 2nd edn, Vol. 2. Part b, pp. 1–19. Springer, Berlin (1962).

The difference of values of c_∞/c_s between hydrogen and oxygen to chlorine and carbon dioxide can be explained qualitatively by considering the difference in solubilities of hydrogen and oxygen to chlorine and carbon dioxide in electrolytes. Although these supersaturation ratios appear to be quite different from each other, the concentration gradients which are the driving force for mass transfer may not be too different.

Glas and Westwater [4] tried to correlate their measured growth coefficient to current density which represents the rate of formation of gas by a so-called "unsteady-state model". The concentration field prior to the formation of the new phase is given by the solution of the diffusion equation [cf. equation (43)]. The concentration at $x = 10^{-3}$ cm was chosen arbitrarily as the hypothetical uniform supersaturation in Scriven's model to calculate the growth coefficient. The waiting time which was not measured was used as an adjustable parameter to fit the data. Better agreement was obtained for cases of chlorine and oxygen.

Using our model, the Jakob number for the case of constant mass flux can be obtained by combining equations (19) and (43),

$$J = \frac{1}{\rho_v}\int_0^\pi [f(0,\theta) - c_s]\sin\theta\,d\theta$$

$$= \frac{1}{\rho_v}\left\{c_\infty + \frac{q}{D}\sqrt{\left(\frac{4Dt}{\pi}\right)} - c_s\right\}. \qquad (52)$$

Taking the example of hydrogen where ρ_v and c_s are the smallest, using waiting periods ranging from 0·02 to 0·2 s and a current density of $3{\cdot}95 \times 10^{-2}$ A/cm²* which corresponds to a mass flux of $4{\cdot}09 \times 10^{-7}$ g equiv/cm² s for the case where the solution is saturated with hydrogen initially, J varies from 0·095 to 0·30. Therefore, it can be concluded that all the observations made by Westwater and coworkers fall exclusively in the case where the convective transport can be neglected. However, since the actual waiting time has not been measured, a quantitative evaluation using our model was not possible.

4. CONCLUSIONS

Theoretical calculations on the dynamics of bubble growth in a nonuniform concentration field were performed. Solutions were obtained for the linear, the exponential concentration fields, the constant interfacial concentration and the constant mass flux cases at both low and high degrees of supersaturation. Unfortunately, no experimental data are available to test these theoretical results.

ACKNOWLEDGEMENTS

The authors wish to thank J. P. Earhart for his assistance with some of the numerical calculations in this work.

This work was performed under the auspices of the United States Atomic Energy Commission.

* These are some typical conditions reported in Glas' work [14].

REFERENCES

1. M. S. PLESSET and S. A. ZWICK, The growth of vapor bubble in superheated liquids, *J. Appl. Phys.* **25**, 493–500 (1954).
2. H. K. FORSTER and N. ZUBER, Growth of a vapor bubble in a superheated liquid, *J. Appl. Phys.* **25**, 474–478 (1954).
3. L. E. SCRIVEN, On the dynamics of phase growth, *Chem. Engng Sci.* **10**, 1–13 (1959)
4. J. P. GLAS and J. W. WESTWATER, Measurement of the growth of electrolytic bubbles, *Int. J. Heat Mass Transfer* **7**, 1427–1443 (1964).
5. L. A. WALDMAN and G. HOUGHTON, Spherical phase growth in superheated liquids, *Chem. Engng Sci.* **20**, 625–636 (1965).
6. P. S. EPSTEIN and M. S. PLESSET, On the stability of gas bubbles in liquid–gas solutions, *J. Chem. Phys.* **18**, 1505–1509 (1950).
7. P. GRIFFITH, Bubble growth rates in boiling, *Trans. Am. Soc. Mech. Engrs* **80**, 721–727 (1958).
8. S. G. BANKOFF, Bubble dynamics at the surface of an exponentially heated plate, *I/EC Fundamentals* **1**, 257–259 (1962).
9. G. BIRKHOFF, R. S. MARGULIES and W. A. HORNING, Spherical bubble growth, *Physics Fluids* **1**, 201–204 (1958).
10. L. A. SKINNER and S. G. BANKOFF, Dynamics of vapor bubbles in spherically symmetric temperature fields of general variation, *Physics Fluids* **7**, 1–6 (1964); Dynamics of vapor bubbles in general temperature fields, *Physics Fluids* **8**, 1417–1420 (1965).
11. H. Y. CHEH, On the mechanism of electrolytic gas evolution, Ph.D. Thesis, UCRL-17324, University of California, Berkeley (1967).
12. H. S. CARSLAW and J. C. JAEGER, *Conduction of Heat in Solids*, 2nd edn. Clarendon Press, Oxford (1959).
13. D. E. WESTERHEIDE and J. W. WESTWATER, Isothermal growth of hydrogen bubbles during electrolysis, *A.I.Ch.E. Jl* **7**, 357–362 (1961).
14. J. P. GLAS, Microscopic growth of electrolytic bubbles, Ph.D. Thesis, University of Illinois, Urbana (1965).

Résumé—Des calculs théoriques sur la dynamique de la croissance asymptotique des bulles sont effectués dans un champ de concentration initialement non-uniforme. Une simplification sensible est réalisée en remarquant que le nombre de Jakob pour le transport de masse est habituellement faible de telle façon que le transport par convection peut être négligé par rapport au transport par diffusion. On a obtenu des solutions numériques pour la vitesse de croissance d'une bulle hémisphérique sur une surface avec des champs de concentration initiaux linéaires et exponentiels du gaz sursaturé dans les couches limites de diffusion et aussi pour les cas où l'on suppose des champs de concentration provenant des expériences à concentration interfaciale constante et à flux de masse constant.

Zusammenfassung—Es werden theoretische Berechnungen durchgeführt über die Dynamik des asymptotischen Anwachsens von Blasen in einem anfänglich ungleichförmigen Konzentrationsfeld. Eine wesentliche Vereinfachung wird durch die Vernachlässigung des konvektiven Transportes gegenüber dem Diffusionstransport erreicht, was bei kleinen Jakob–Zahlen für Stofftransport gewöhnlich möglich ist. Numerische Lösungen werden erhalten für die Anwachsgeschwindigkeit einer halbkugeligen Blase an einer Oberfläche mit linearer oder exponentieller Anfangsverteilung des Konzentrationsfeldes des überhitzten Gases in der Diffusionsgrenzschicht, sowie für die Fälle, dass sich Konzentrationsfelder aus konstanten Zwischenschichtkonzentrationen ergeben, und dass der Massenstrom konstant ist.

Аннотация—Проведен теоретический расчет динамики асимптотического роста пузырьков в полях концентрации с начальной неоднородностью. Достигается значительное упрощение, если учесть, что число Якоба для массообмена обычно мало, так что конвективным переносом по сравнению с диффузионным можно пренебречь. Получены численные решения для скорости роста полусферического пузырька на поверхности с исходными линейными и экспоненциальными полями концентрации перенасыщенного газа в диффузионных пограничных слоях, а также для случаев наличия полей концентрации, возникающих в экспериментах при постоянной концентрации на поверхности раздела фаз и постоянном массовом потоке.